Journal of Studies in Science and Engineering

EngiScience Publisher

Review Article

Compact Multiband Circularly Polarized Filtering Antenna

Kiran Sonawane [1,*], Pravin Patil [2]

[1] Electronics and Telecommunication, RC Patel Institute of Technology, Shirpur, 425405, India

[2] Electronics and Telecommunication Engineering, SSVPSBSD College of Engineering, Dhule, 424005, India

*Corresponding Author: Kiran Sonawane, E-mail: khsona2009@email.com

Article Info

Article History

Received Apr 05, 2024

Revised May 18, 2024

Accepted Jun 22, 2024

Keywords

Circularly Polarised Antenna

Filtering Antenna

Impedance Bandwidth

Biomedical Applications

Codesign Circuit

FR4

5G

Abstract

A miniature circularly polarised filtering antenna device is presented here. The device has an impeccably circular radiating patch coupled with pins to stripline circuits with open-loop ring resonators. In the proposed design, the filter's last stage acts as a radiating patch and has a low profile of 0.57λ0 x 0.57λ0 x 0.07λ0 at a centre frequency of 4.26 GHz. The codesigned filtering circuit improves the wide impedance bandwidth and axial ratio of 3 dB bandwidth. The filtenna was designed, fabricated and measured, gaining more than 2.5 dB and S11< -14 dB for an impedance bandwidth of 700 MHz from 4.1 to 4.8 GHz. Impedance bandwidth, which is needed for wireless applications, is 13.33%. The developed circularly polarised codesign filtering antenna was verified using full wave models and testing. The filtering antenna is useful for biomedical applications such as wearable and 5G applications.

1. Introduction

The integration of microwave components has become necessary where size reduction and increased overall performance are concerned, as wireless communication technology is improving daily. Any antenna design requires antenna and filter circuits, vital elements in the design process [1]. The antenna handles signal transmission and reception, while the frontend circuit, known as the bandpass filter, separates the desired signal [2-4]. The quality of the S11 and antenna gain is impaired by interference since the antenna and BPF are resonating simultaneously. If the impedance is not correctly synched, the enactment of the antenna will be adversely impacted, for example, by 50 or 75Ω over the bandwidth or at the band edges. Recent work has focused on codesigning BPF and antenna for a single device. The final stage of filter design provides the ultimate solution, which behaves as an antenna radiator as an electromagnetic bandgap antenna [5]. To acquire good bandwidth, several filtering antennas were tested. In several existing literature,

antennas were used as dispersive complex loads in filter circuits for wire monopoles and horn antennas [6], wire monopoles [7], coupled planar resonator connected patch antenna [8, 9], SIW resonators with coaxial collinear antennas [10]. A hybrid feeding methodology with integrated stripline and air-filled substrate waveguide structures creates a circularly polarised antenna array [1]. In Cameron, et al. [2], a small footprint single-layer circularly polarised patch antenna is built. The wideband circularly polarised 2x2 filtering was obtained in Hong and Lancaster [3] with increased gain and AR bandwidth. In codesign, the last stage of BPF acts as an antenna having coupled sub-strate-integrated waveguide cavity filters cascaded to slot antenas [11-14] and planar monopole antennas combined with coupled line filters [15-17].

Due to their applications in wireless communications, which hold enormous potential for bio-medical fields, battlefield survival, and patient tracking systems, wearable antenna, one of the fastest evolving fields in the antenna community, has attracted research interest worldwide [18, 19]. Different types of wearable antennas were developed on HSCA and PICA [20], IFA [21], planer microstrip monopoles [22-24], PIFA [25, 26], slot antenna [27], stepped impedance resonator antenna [28], patch antennas [29], cavity backed slot antenna [30, 31] having broadside radiation pattern. Artificial magnetic conducting surfaces [32-34] and metasurface [35-37] have small isolation profiles between antenna and human tissues.

In this paper, we focus on two major issues, narrow operating band and multiband operations, by introducing an innovative approach for compact codesign CP filtenna, without adjusting the size. In section 2, we described the methodology of circularly polarised filtenna by elucidating the 3D design, equivalent circuit, and structural design of the antenna and filter. Section 3 describes the simulation and measurement outcomes in air. Also, the final CP codesign is compared with rectangular and cross-ring resonators, followed by conclusions in section 4.

2. Methodology

The codesign CP filtenna is vertically assembled and connected using a metallised via hole portrayed in Figure 1, having a rounded patch radiator on the top layer and a planer dual stripline microwave circuit on the bottom layer consisting of filtering, phase splitting, power disparities and conjugate matching functions required to radiate CP wave. The filter circuit is sandwiched in the middle and shared by both path and ground plane. This configuration significantly reduces the device's size. Optimising via hole location and dimensions improves impedance at interferences, enhancing performance. Two bandpass filters were

connected to circular radiating patch through a coupled stripline & two metallic pins that passed through the ground plane between the top and middle layers. The two metallic pins were located at some offset from the centre of the circular radiating patch to obtain good impedance matching. The bottom ground plane of the circular patch radiator (top layer) acts as the top ground plane of the stripline circuit (middle layer). Two bandpass filter circuits consist of three open-loop ring resonators, which are mutually coupled to one another. SMA connector was connected to the bandpass filter with the top and bottom ground connected from the side instead of the bottom side, as discussed in wearable medical uses [37]. The BPF design comprises three rectangular open-loop edge coupled resonators [38]. The size of filtenna is 40 mm x 40 mm x 5.3 mm (0.57λ0 x 0.57λ0 x 0.07λ0) where λ0 =70.42 mm at centre frequency 4.26 GHz, which is compact as compared to other filtering antennas [4-6]. A ring resonator filtering antenna multi-layer antenna array has been chosen to satisfy the abovementioned criteria. An RT/Duroid 5880 with εr =2.2 a thickness of 0.79 mm, and tanδ =0.0009 was used for prototype design.

The radius of the patch is the only parameter to control the resonant frequency. The radius of the patch (a) can be determined by

$$a = \frac{F}{\sqrt{1+\frac{2h}{\pi \epsilon r F\left[\ln\left(\frac{F\pi}{2h}\right)+1.7726\right]}}} \tag{1}$$

where

$$F = \frac{8.791\times10^{9}}{f_r \times \epsilon r} \tag{2}$$

The patch radius is calculated using parameters h= 3.68 mm, εr = 2.2, F=1.3912 in equation (1) and (2) the radius (a) is 1.391 cm=13.91 mm, h = height of substrate, εr = dielectric constant of the substrate. Guided Wavelength is given by

$$\lambda_g = \frac{300}{f(GHz)\sqrt{\varepsilon_r}} = \frac{300}{4.26\sqrt{2.2}} = 47.47mm \tag{3}$$

The radius of the ring resonator is given by

$$r = \frac{\lambda_g}{2\pi} = \frac{47.47}{2\pi} = 7.55mm \tag{4}$$

At fundamental frequency, the ring is resonated when a mean circumference

$$2 \times \pi \times r \approx \lambda_g = 2 \times \pi \times 8.047 = 50.56mm$$

The layout is represented in Figure 1, where three substrate layers have heights of h1=3.68, h2=0.79,

and h3=0.79, all in millimetres.

The analogous circuit for CP filtenna is publicised in Figure 2. A shunt equivalent circuit (Rx, Lx, Cx or Ry, Ly, Cy) was used for the orthogonal model [39]. The inductance of the feeding pin was represented by a series inductor. The three parallel RLC resonators depict the three open loop ring resonators (OLRR) synchronously/asynchronously tuned. An admittance inverter was used to couple stages [40]. Striplines were capacitively coupled, and the third resonator connected to a circular radiating patch in each filter-branch is represented as an admittance inverter with a transmission line [41]. For circular polarisation, two filtering branches were connected to the T section with an electrical length of λ/4 for impedance matching, which also gives a 90° phase difference—a quarter-wave transformer was employed for impedance matching of the input impedance of 50ohm at the T junction of antenna port.

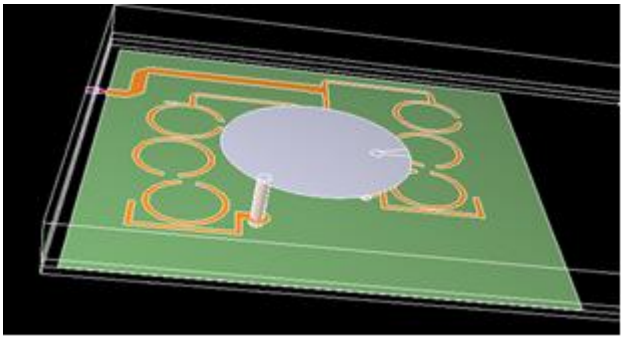

Figure 1. 3D view of CP filtenna using an open loop resonator with a stripline feed

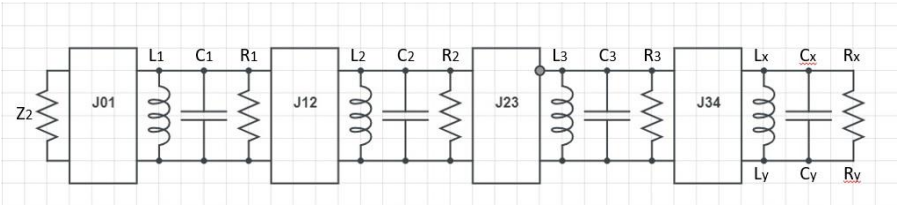

Figure 2. Equivalent circuit of CP filtenna

The BPF was designed to have a fractional bandwidth of 13.33% at 4.26 GHz. We selected a four-pole (n=4) Chebyshev LPF prototype with a passband ripple of 0.2 dB and 50-ohm impedance. The LPF parameter includes g_0=1, g_1=1.303, g_2=1.284, g_3=1.976, g_4=0.847, g_5=1.539 [2, 3].

For low pass normalisation, to get the actual component values, the following equations [3] are used

$$C_n = \frac{G_n}{2\pi f_c R} \tag{5}$$

$$L_n = \frac{G_n R}{2\pi f_c} \tag{6}$$

Using equation (5) & (6) we can find values of C_1=0.608pf, C_2=0.599pf, C_3=0.922pf, L_1=3.89nH,

L_2=3.8nH, L_3=5.90nH, R_1=R_2=R_3=0.649Ω, Z_{BPFi}=Z_2=80Ω. The IE3D was used to simulate the pin-fed patch antenna alone by adjusting the diameter of the circular patch, thickness of the top substrate layer, position of the feeding pin, input resistance, and optimum antenna performance obtained. The AR was below 3dB throughout this 13.33% fractional bandwidth, indicating good matching. The antenna is the last stage of the filter's resonator and acts as a patch radiator. Based on the low-pass parameters, the designed parameters for the bandpass filter are as follows:

The external quality factor

$$Q_{e1} = \frac{g_0 g_1}{FBW}, \quad Q_{en} = \frac{g_n g_{n+1}}{FBW} \tag{7}$$

$$Q_e = \frac{g_1}{FBW} = \frac{1.303}{0.1333} = 9.774 \tag{8}$$

Coupling coefficients for filters can be determined by

$$M_{i,i+1} = M_{n-i,n-i+1} = \frac{FBW}{\sqrt{g_i g_{i+1}}} \; for \; i = 1,2,\ldots\ldots,\frac{n}{2} - 1 \tag{9}$$

$$M_{12} = M_{34} = \frac{0.1333}{\sqrt{1.303 \times 1.284}} = 0.090$$

and

$$M_{i,n+1-i} = \frac{FBW.J_i}{g_i} \; for \; i = 1,2,\ldots\ldots,\frac{n}{2} \tag{10}$$

$$M_{23} = \frac{0.1333 \times 0.8012}{1.284} = 0.083$$

where Q_{e1} and Q_{en} are the external quality factors of the resonators at the input and output port and $M_{i,i+1}$ are the coupling coefficients between the i^{th} and $(i+1)^{th}$ resonator, and n is the order of the filter. The resistance of each BPF acts as purely resistive. At the T-shaped junction, two branches converge to have a feed patch with a quadrature phase to realise circular polarisation. A $\lambda/4$ (quarter-wave transformer) is formed to synch impedance of 50ohm at the antenna port. Two identical BPF was designed so that band-width should be enhanced with filtering & impedance matching functions. Consider the electrical length of $\lambda/4$ at fc and characteristic impedance of 80 Ohm to obtain the desired performance. At centre frequency, the coupled stripline's length should be approximately one-quarter wavelength, which is 12.6 mm. The separation distance was 0.21 mm using equation [41]. Wide bandwidth was obtained by using two LPFs joined to T junction. The two planer striplines have a length difference of around 12.6 mm, which is $\lambda/4$ of fc. Over 13.33% bandwidth, a quarter wavelength stripline provides the desired 90° phase shift. In our design's optimised dimensions of the proposed filter are shown in Table 1.

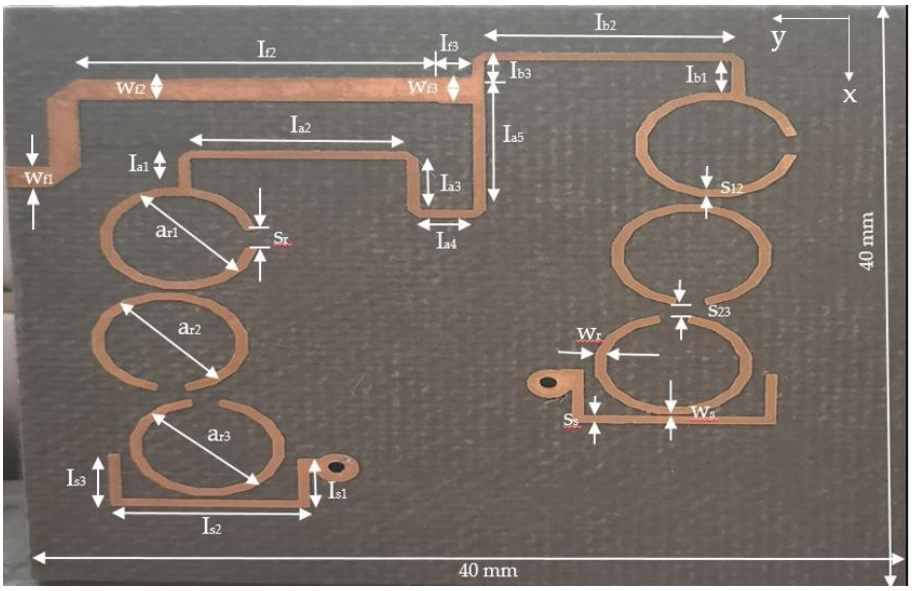

Figure 3. Top view of stripline BPF layer

Table 1. Final dimensions of ring resonator design

ar1	ar2	ar3	br	sr	wr	s12	s23	ss
7	7	7	7.6	1.5	0.5	0.5	0.525	0.21
ws	Is1	Is2	Is3	t	Ia1	Ia2	Ia3	Ia4
0.15	3.5	9	3.7	3.7	2	9.4	3.4	2.4
Ia5	Ib1	Ib2	Ib3	If2	If3	wf1	wf2	wf3
2.4	2	10.5	1.1	11.2	2	1.35	1.47	1.73

3. Results and Discussions

The proposed circularly polarised BPF was experimentally designed and simulated in IE3D EM simulation software. The simulated S11 is depicted in Figure 4 in solid line where optimised design has below -14 dB, and fractional bandwidth is 13.33%, for passband having centre frequency 4.26 GHz. The S11 for complete geometry consists of two low pass filter circuits, a phase shifter, a power divider and conjugate matching circuits shown in Figure 3. The simulation radiation efficiency in the passband was more than 80%, as shown in Figure 8. The simulated geometry has a fourth-order Chebyshev BPF response. The AR shown in Figure 9 is less than 3 dB for the frequency range, from 4 GHz to 4.8 GHz, which indicates the quality and reliability of the design. The S11<-14 dB for the frequency range from 4.1 GHz to 4.8 GHz. The important dimensional parameters for tuning have sizes of all SOLRs, the gap/distance between adjacent SOLRs, the diameter of patch radiator, feed point of pins, the position of tapping strip line, and length, width and spacing of coupled strip traces.

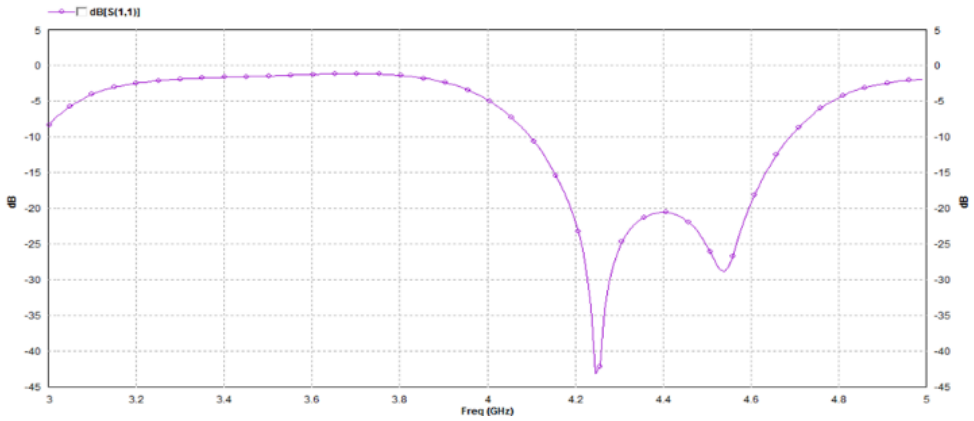

Figure 4. Simulation result of CP filtering antenna using final ring resonator design

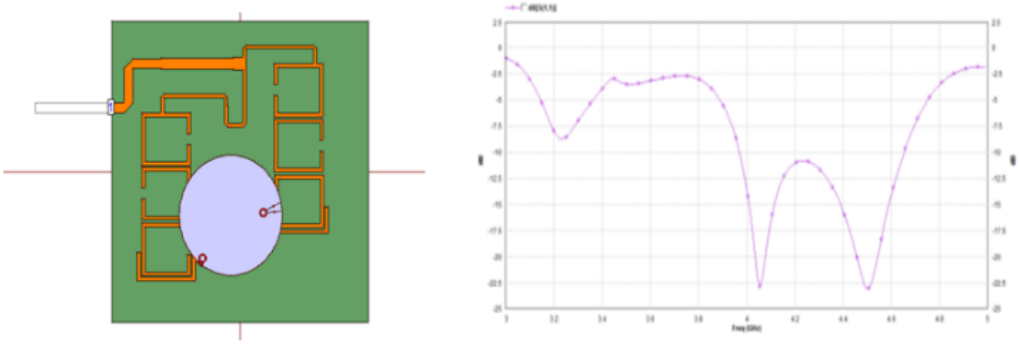

(a) Simulation result of CP filtering antenna using rectangular resonator

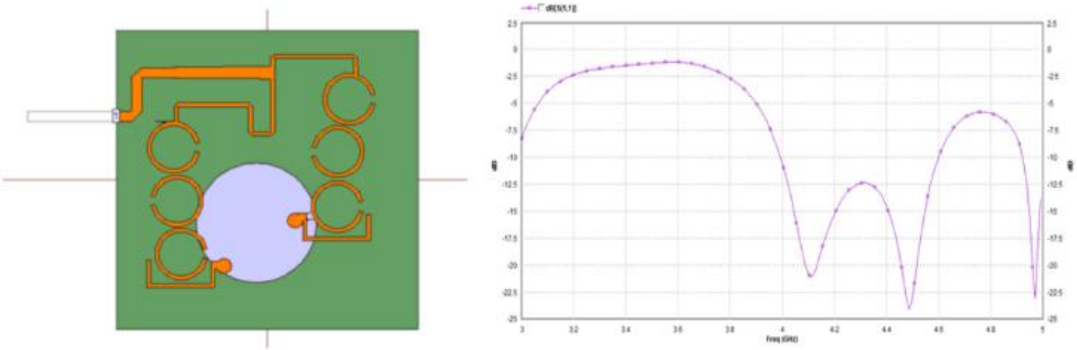

(b) Simulation result of CP filtering antenna using a cross-ring resonator

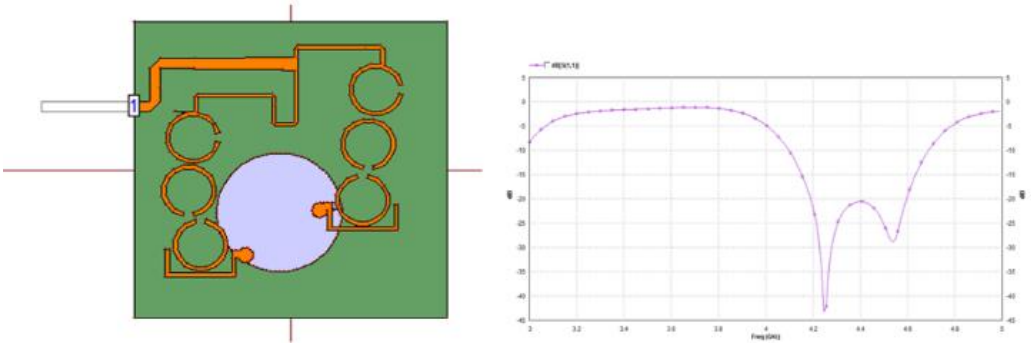

(c) Simulation result of CP filtering antenna with a final ring resonator

Figure 5. Simulation result of different combinations of CP filtering antenna.

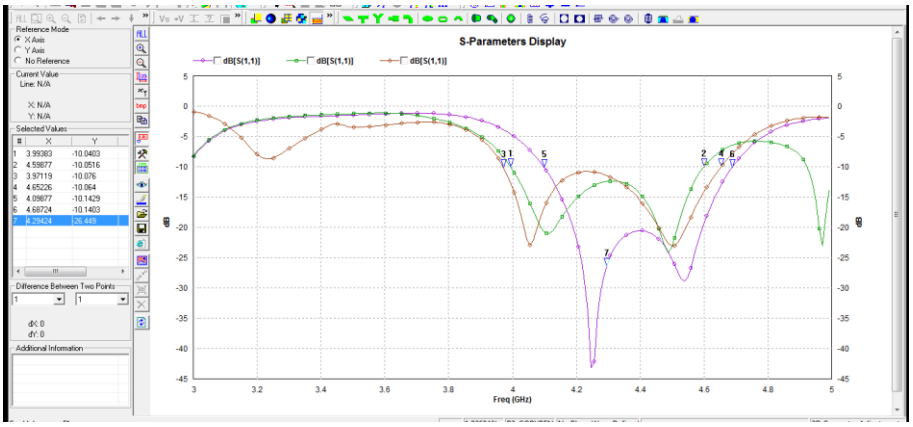

Figure 6. Simulation results of the rectangular resonator, ring resonator and final ring resonator designs

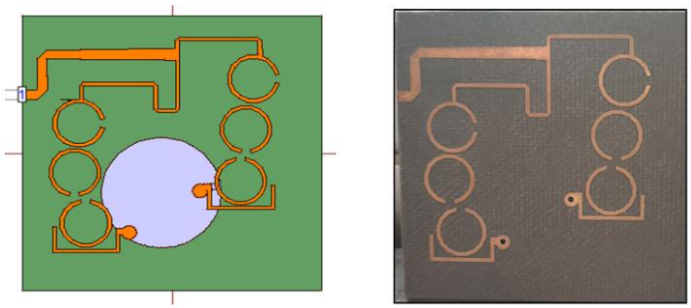

(a) (b)

Figure 7. Top view of stripline BPF layer a) Simulation Design b) Prototype BPF

Suppose there is mismatching between two branches of the low pass filter and the T junction, increasing AR values. Wideband CP filtenna can be obtained using other techniques using thick air substrates [42], dual feeding with planer hybrid coupler [43], and defective ground structure broadband 90° baluns [39], but all other methods require more thickness. Integrating filtering and antenna may raise the size of the antenna, which is not compact enough for some wireless applications. To obtain optimum result at resonant frequency, the radius of the radiating patch antenna is 8 mm with modification to be Q_{ei}=9.28, Q_{eo}-10.02, M_{12}=0.106, M_{23}=0.086 and M_{34}=0.107 to obtain the desired filtering performance.

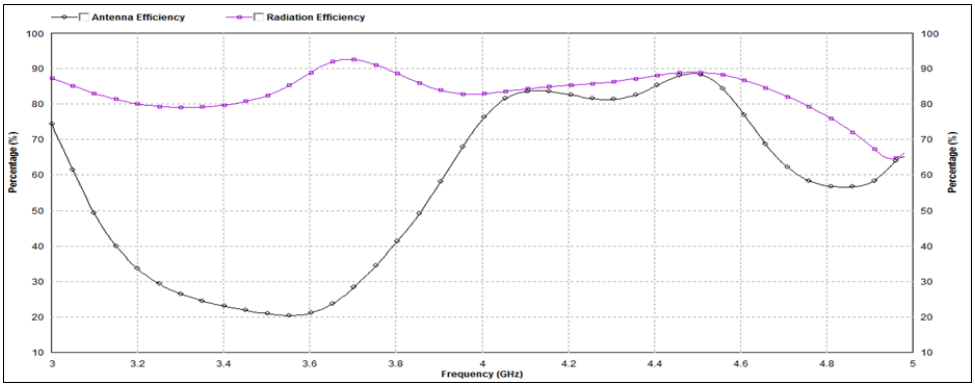

Figure 8. Radiation and antenna efficiency of CP filtering antenna

Figure 8 shows the radiation efficiency of the CP filtering antenna, which is 81.65% and antenna efficiency is 81.62% at resonance 4.24GHz and 76.96% and 77.07% at resonance frequency 4.53GHz. Using the standard method and the final prototype modules, a CP filtering antenna was fabricated on an RT/Duroide 5880 PCB. An SMA connector was attached to the planer stripline with a ground terminal to both (lower and upper) ground layers. Figure 11(a, b) shows photographs of the top and back view of the final fabricated and assembled CP antenna modules consisting of three layers.

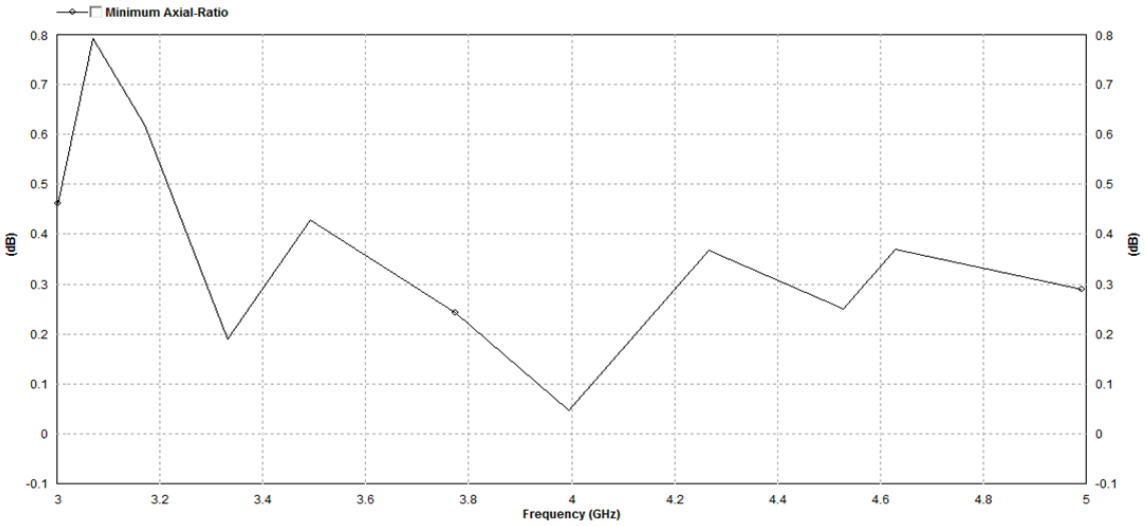

Figure 9. The axial ratio of the CP filtering antenna

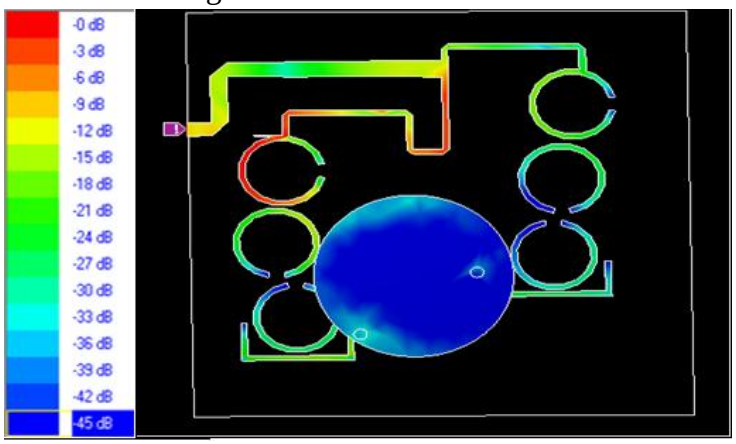

Figure 10. Current simulation of CP filtering antenna

Figure 10 shows the current distribution. The current is non-uniformly distributed at a frequency of 4.26 GHz, where resonance occurs, as shown in the figure above. The majority of the current flows through the left-side bandpass filter. It is seen that the surface current distribution is at 4.26 and 4.65 GHz, and the surface current density is mainly concentrated around the hybrid microstrip coplanar waveguide in the ring resonator, as shown in Figure 10.

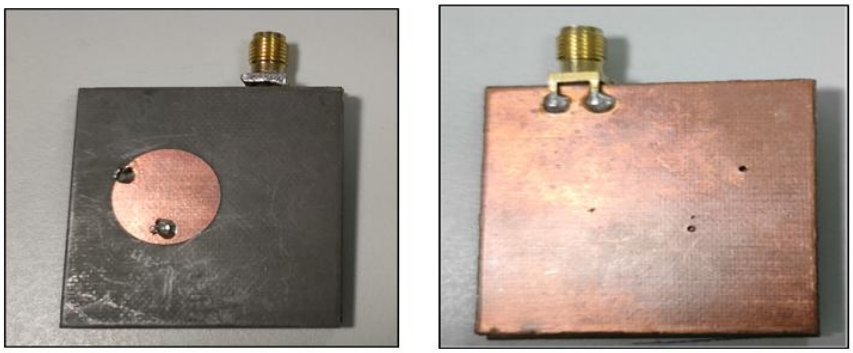

Figure 11. Photographs of the final module (a) Top View, (b) Back View

RHODE & SCHWARZ ZVL network analyser was used to measure the impedance of CP filtering antennas. As shown in Figure 12, measured S11 of CP filtenna exhibits good filtering properties with S11< -13.33dB within 4.06 GHz to 4.64 GHz. The slight variations in the simulated and measured band S11 and slightly decreased roll-offs are due to fabrication and assembly inaccuracies; the slight reflection coefficient response shifted to higher frequencies and broadened. Such a minor blue shift and band broadening can also be observed in the measured reflection coefficient (see Figure 12). For comparison with previously reported, Table 2 includes information on footprint, antenna profile, S11, pattern type, polarisation, and bandwidth. The performance of this work is superior to that of previous works.

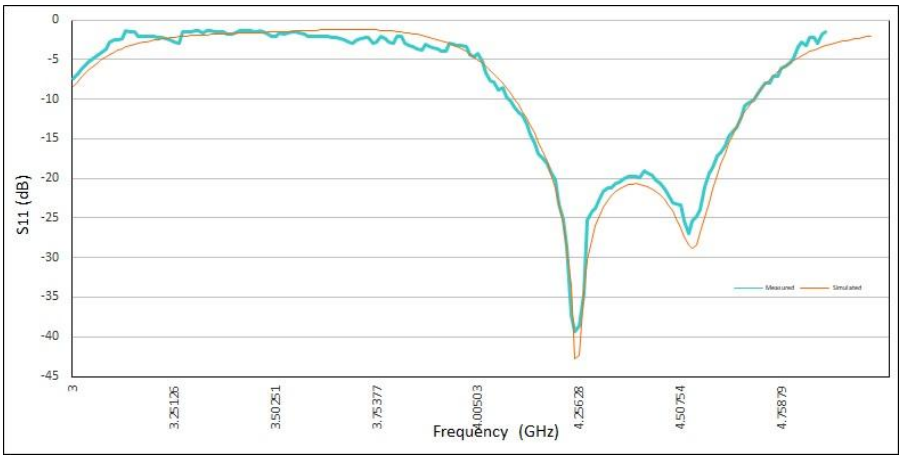

Figure 12. Simulated and measured S11.

Figure 13 shows the 2D radiation pattern at 4.26 GHz and 4.65 GHz in both the x-y and x-z patterns. The main beam is slightly shifted from the broadside due to offset pin feed concerning the centre of the patch and offset patch position away from the centre of the ground plane. They have nearly equal HPBW of 73˚ and 74 ˚ in x-y and x-z planes. The gain is nearly the same (i.e., 2.53 Db) at 4.26 GHz and 4.65 GHz. The wide HPBW is favoured for angular coverage.

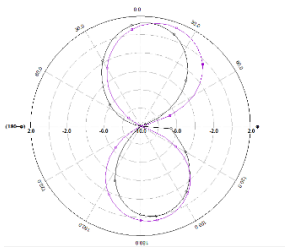

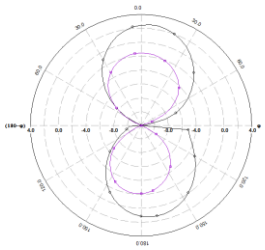

4.26GHz (a) 4.65GHz

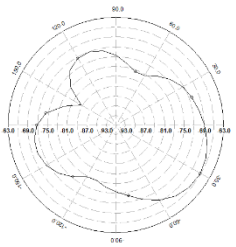

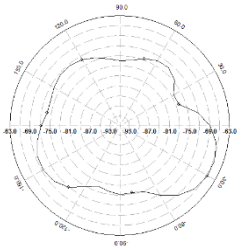

4.26GHz (b) 4.65GHz

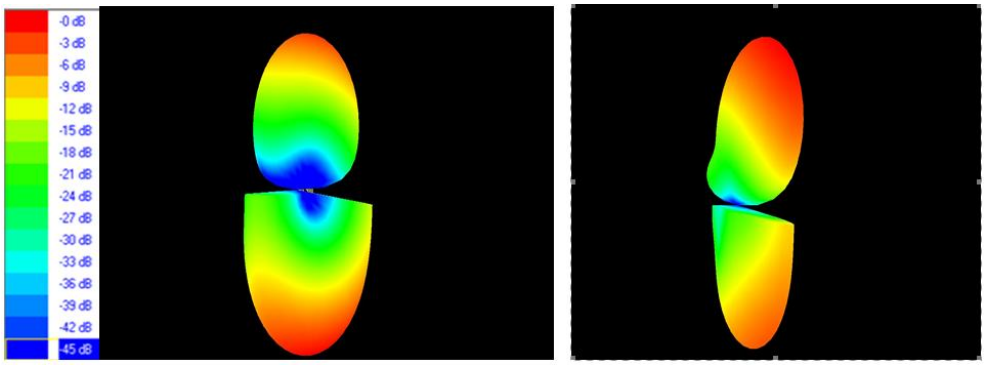

(c)

Figure 13. 2D radiation pattern at (a)x-y,(b)x-z plane and (c) 3D radiation pattern

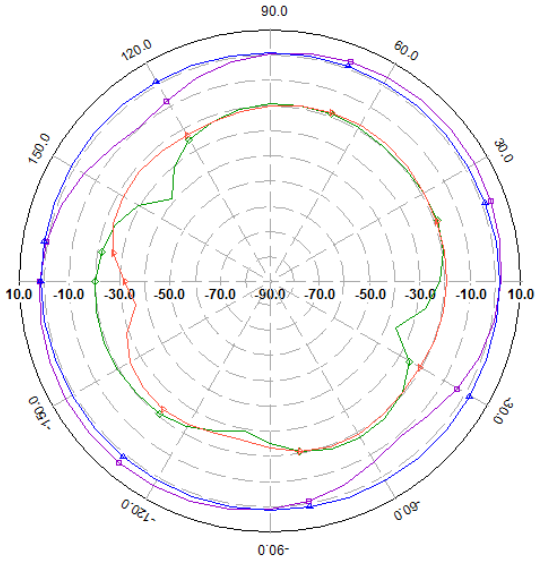

Figure 14. Co-polarisation and cross polarisation at a)4.26GHz and b)4.65GHz.

The normalised far-field pattern in both the x-z and y-z planes is shown in Figure 14; for circular polarisation, the axial ratio (AR) should be one or less than 1. In Figure 14, purple and blue lines indicate co-polarisation at 4.26 and 4.65 GHz respectively, and green and orange lines indicate cross-polarisation at 4.26 and 4.65 GHz. The main beam is slightly shifted due to the offset pin fed concerning the centre of the patch, and the offset patch shifted from the centre of the ground plane. To verify the performance of the filtering antenna, compare previously reported antenna with antenna properties codesign, footprint, antenna profile, S11 bandwidth, gain, radiation efficiency, polarisation and pattern in Table 2.

Table 2. Simulation results and experimental validation

Ref	Codesign	Footprint	Profile	S11 BW	Gain	Rad. Efficiency	Polarisation	Pattern
[4]	Yes	13.7	>3	5.5% (-13 dB)	17	50%	Linear	Highly Directive
[5]	No	3.5	>3	9.8% (-14 dB)	NA	79%	Linear	Highly Directive
[6]	No	7.2	2.5	6.3% (-10 dB)	14	90%	Circular	Highly Directive
[7]	No	3.01	1.7	7.7% (-10 dB)	NA	74%	Linear	Omnidirectional
[8]	No	0.36	0.02	4.7% (-10 dB)	4.3	50%	Linear	Unidirectional
[9]	No	0.2	0.45	4.5% (-10 dB)	3.5	58%	Circular	Unidirectional
[10]	No	3.6	0.05	2.6% (-10 dB)	7.8	78%	Linear	Omnidirectional
[11]	Yes	0.43	0.02	2.5% (-10 dB)	4.87	NA	Linear	Unidirectional
[12]	Yes	1.56	0.1	6.1% (-15 dB)	6.1	89%	Linear	Unidirectional
[13]	Yes	0.39	0.15	3% (-14 dB)	4.9	59%	Linear	Unidirectional
[14]	Yes	0.32	0.01	13% (-10 dB)	0.65	74%	Linear	Omnidirectional
[15]	Yes	1.17	0.01	3% (-12 dB)	9.6	72%	Linear	Highly Directive
[16]	Yes	0.25	0.01	2% (-13 dB)	-3	NA	Linear	Unidirectional
[43]	Yes	0.28	0.07	12.5% (-14 dB)	5.2	80%	Circular	Unidirectional
This Work	Yes	0.28	0.07	13.33% (-14 dB)	2.75	81.65%	Circular	Unidirectional

4. Conclusions

We proposed a novel design scheme of compact, wide impedance bandwidth CP filtenna having two LPF branches has been presented. The codesign of the antenna and BPF circuit using a circular radiating patch as a load of open loop ring resonators. A proposed filtenna has a thickness of 5.3 mm and a smaller size of 40 mm x 40 mm. A compact multiband CP filtenna operating at 4.26 GHz has been designed, fabricated and validated. The proposed antenna achieves a measured S11= -14dB bandwidth of 13.33% and a peak gain of 2.75 dBi, with AR smaller than 3dB and a maximum efficiency of 81.65%. By optimising

various antenna characteristics, remarkable optimal results were achieved compared to the most recent literature. Measured results confirmed that the proposed antenna is an opponent for real-time applications such as 5G applications (4.4–4.9) GHz, Unmanned aerial vehicles (4.4 to 4.5) GHz applications and (4.635 to 4.685) GHz for radar information distribution networks and wearable devices for biomedical applications.

Acknowledgement*:* The authors wish to acknowledge the Rogers Corporation for providing RT/duroid 5880 material and shipping at no charge.

Declaration of Competing Interest The authors declare that they have no known competing of interest.

References

[1] D. M. Pozar, *Microwave and RF design of wireless systems*. John Wiley & Sons, 2000.

[2] R. J. Cameron, C. M. Kudsia, and R. R. Mansour, *Microwave filters for communication systems: fundamentals, design, and applications*. John Wiley & Sons, 2018.

[3] J.-S. G. Hong and M. J. Lancaster, *Microstrip filters for RF/microwave applications*. John Wiley & Sons, 2004.

[4] B. Herdiana, "Comparative Analysis of Multi-Substrate Materials in Microstrip Antenna Models for Broadband Wireless Communications," *International Journal of Electronics and Communications*, vol. 2, no. 1, pp. 1-7, 2022.

[5] N. Chahat, M. Zhadobov, L. Le Coq, S. I. Alekseev, and R. Sauleau, "Characterization of the interactions between a 60-GHz antenna and the human body in an off-body scenario," *IEEE Transactions on Antennas and Propagation*, vol. 60, no. 12, pp. 5958-5965, 2012.

[6] G. Q. Luo *et al.*, "Filtenna consisting of horn antenna and substrate integrated waveguide cavity FSS," *IEEE transactions on antennas and propagation*, vol. 55, no. 1, pp. 92-98, 2007.

[7] H. Zhou *et al.*, "Filter-antenna consisting of conical FSS radome and monopole antenna," *IEEE Transactions on Antennas and Propagation*, vol. 60, no. 6, pp. 3040-3045, 2012.

[8] J. Zuo, X. Chen, G. Han, L. Li, and W. Zhang, "An integrated approach to RF antenna-filter co-design," *IEEE Antennas and Wireless Propagation Letters*, vol. 8, pp. 141-144, 2009.

[9] Z. H. Jiang, M. D. Gregory, and D. H. Werner, "Design and experimental investigation of a compact circularly polarized integrated filtering antenna for wearable biotelemetric devices," *IEEE Transactions on Biomedical Circuits and Systems*, vol. 10, no. 2, pp. 328-338, 2015.

[10] C. Yu, W. Hong, Z. Kuai, and H. Wang, "Ku-band linearly polarized omnidirectional planar filtenna," *IEEE Antennas and Wireless Propagation Letters*, vol. 11, pp. 310-313, 2012.

[11] O. A. Nova, J. C. Bohorquez, N. M. Pena, G. E. Bridges, L. Shafai, and C. Shafai, "Filter-antenna module using substrate integrated waveguide cavities," *IEEE Antennas and Wireless Propagation Letters*, vol. 10, pp. 59-62, 2011.

[12] Y. Yusuf and X. Gong, "Compact low-loss integration of high-$ Q $3-D filters with highly efficient antennas," *IEEE transactions on microwave theory and techniques*, vol. 59, no. 4, pp. 857-865, 2011.

[13] Y. Yusuf, H. Cheng, and X. Gong, "A seamless integration of 3-D vertical filters with highly efficient slot antennas," *IEEE Transactions on Antennas and Propagation*, vol. 59, no. 11, pp. 4016-4022, 2011.

[14] K. Sonawane and P. Patil, "Multiband Slot Antenna with DGP for Future Wireless Applications," in *2022 International Conference on Industry 4.0 Technology (I4Tech)*, 2022, pp. 1-5: IEEE.

[15] C.-T. Chuang and S.-J. Chung, "Synthesis and design of a new printed filtering antenna," *IEEE Transactions on Antennas and Propagation,* vol. 59, no. 3, pp. 1036-1042, 2011.

[16] C.-K. Lin and S.-J. Chung, "A filtering microstrip antenna array," *IEEE transactions on microwave theory and techniques,* vol. 59, no. 11, pp. 2856-2863, 2011.

[17] C.-K. Lin and S.-J. Chung, "A compact filtering microstrip antenna with quasi-elliptic broadside antenna gain response," *IEEE Antennas and wireless propagation letters,* vol. 10, pp. 381-384, 2011.

[18] P. S. Hall and Y. Hao, *Antennas and propagation for body-centric wireless communications*. Artech house, 2012.

[19] C. C. Poon, B. P. Lo, M. R. Yuce, A. Alomainy, and Y. Hao, "Body sensor networks: In the era of big data and beyond," *IEEE reviews in biomedical engineering,* vol. 8, pp. 4-16, 2015.

[20] P. S. Hall *et al.*, "Antennas and propagation for on-body communication systems," *IEEE Antennas and Propagation Magazine,* vol. 49, no. 3, pp. 41-58, 2007.

[21] Y. Nechayev, P. Hall, and Z. Hu, "Characterisation of narrowband communication channels on the human body at 2.45 GHz," *IET Microwaves, Antennas & Propagation,* vol. 4, no. 6, pp. 722-732, 2010.

[22] M. Suma, P. Bybi, and P. Mohanan, "A wideband printed monopole antenna for 2.4-GHz WLAN applications," *Microwave and Optical Technology Letters,* vol. 48, no. 5, pp. 871-873, 2006.

[23] H.-D. Chen, J.-S. Chen, and Y.-T. Cheng, "Modified inverted-L monopole antenna for 2.4/5 GHz dual-band operations," *Electronics letters,* vol. 39, no. 22, pp. 1567-1568, 2003.

[24] Z. Wang, L. Z. Lee, D. Psychoudakis, and J. L. Volakis, "Embroidered multiband body-worn antenna for GSM/PCS/WLAN communications," *IEEE Transactions on Antennas and Propagation,* vol. 62, no. 6, pp. 3321-3329, 2014.

[25] P. J. Soh, G. A. Vandenbosch, S. L. Ooi, and N. H. M. Rais, "Design of a broadband all-textile slotted PIFA," *IEEE Transactions on Antennas and Propagation,* vol. 60, no. 1, pp. 379-384, 2011.

[26] Q. Bai and R. Langley, "Crumpling of PIFA textile antenna," *IEEE Transactions on Antennas and Propagation,* vol. 60, no. 1, pp. 63-70, 2011.

[27] M. V. Varnoosfaderani, D. V. Thiel, and J. W. Lu, "A folded slot antenna with full ground plane for wearable waterproof wireless sensors," in *2014 IEEE Antennas and Propagation Society International Symposium (APSURSI)*, 2014, pp. 838-839: IEEE.

[28] M. V. Varnoosfaderani, D. V. Thiel, and J. Lu, "External parasitic elements on clothing for improved performance of wearable antennas," *IEEE Sensors Journal,* vol. 15, no. 1, pp. 307-315, 2014.

[29] A. Alomainy *et al.*, "Statistical analysis and performance evaluation for on-body radio propagation with microstrip patch antennas," *IEEE Transactions on Antennas and Propagation,* vol. 55, no. 1, pp. 245-248, 2007.

[30] N. Haga, K. Saito, M. Takahashi, and K. Ito, "Characteristics of cavity slot antenna for body-area networks," *IEEE Transactions on Antennas and Propagation,* vol. 57, no. 4, pp. 837-843, 2009.

[31] S. Agneessens and H. Rogier, "Compact half diamond dual-band textile HMSIW on-body antenna," *IEEE Transactions on Antennas and Propagation,* vol. 62, no. 5, pp. 2374-2381, 2014.

[32] S. Zhu and R. Langley, "Dual-band wearable textile antenna on an EBG substrate," *IEEE transactions on Antennas and Propagation,* vol. 57, no. 4, pp. 926-935, 2009.

[33] H. R. Raad, A. I. Abbosh, H. M. Al-Rizzo, and D. G. Rucker, "Flexible and compact AMC based antenna for telemedicine applications," *IEEE Transactions on antennas and propagation,* vol. 61, no. 2, pp. 524-531, 2012.

[34] S. Yan, P. J. Soh, and G. A. Vandenbosch, "Low-profile dual-band textile antenna with artificial magnetic conductor plane," *IEEE Transactions on Antennas and Propagation,* vol. 62, no. 12, pp. 6487-6490, 2014.

[35] Z. H. Jiang, D. E. Brocker, P. E. Sieber, and D. H. Werner, "A compact, low-profile metasurface-enabled antenna for wearable medical body-area network devices," *IEEE Transactions on antennas and propagation,* vol. 62, no. 8, pp. 4021-

4030, 2014.

[36] C. Hertleer, H. Rogier, L. Vallozzi, and L. Van Langenhove, "A textile antenna for off-body communication integrated into protective clothing for firefighters," *IEEE Transactions on Antennas and Propagation,* vol. 57, no. 4, pp. 919-925, 2009.

[37] E. K. Kaivanto, M. Berg, E. Salonen, and P. De Maagt, "Wearable circularly polarized antenna for personal satellite communication and navigation," *IEEE Transactions on Antennas and Propagation,* vol. 59, no. 12, pp. 4490-4496, 2011.

[38] J.-S. Hong and M. J. Lancaster, "Couplings of microstrip square open-loop resonators for cross-coupled planar microwave filters," *IEEE Transactions on Microwave theory and Techniques,* vol. 44, no. 11, pp. 2099-2109, 1996.

[39] Z. H. Jiang and D. H. Werner, "A compact, wideband circularly polarized co-designed filtering antenna and its application for wearable devices with low SAR," *IEEE Transactions on Antennas and Propagation,* vol. 63, no. 9, pp. 3808-3818, 2015.

[40] L. Zhu, *Microwave Bandpass Filters for Wideband Communications*. Wiley, 2011.

[41] M. P. David, "Microwave Engineering, ; Joihn Wiley & Sons," *Inc.: Hoboken, NJ, USA*, 2012.

[42] X. Qing, "Broadband aperture-coupled circularly polarized microstrip antenna fed by a three-stub hybrid coupler," *Microwave and optical technology letters,* vol. 40, no. 1, pp. 38-41, 2004.

[43] Y.-X. Guo, K.-W. Khoo, and L. C. Ong, "Wideband circularly polarized patch antenna using broadband baluns," *IEEE Transactions on Antennas and Propagation,* vol. 56, no. 2, pp. 319-326, 2008.